HMG Advance Access published February 23, 2011

Human Molecular Genetics, 2011 **1–13**
doi:10.1093/hmg/ddr049

Expanded polyglutamine domain possesses nuclear export activity which modulates subcellular localization and toxicity of polyQ disease protein via exportin-1

Wing Man Chan[1,3,4,†], Ho Tsoi[1,4,†], Chi Chung Wu[1,3], Chi Hang Wong[5], Tat Cheung Cheng[1,3], Hoi Yeung Li[5], Kwok Fai Lau[2,3,4], Pang Chui Shaw[4], Norbert Perrimon[6] and Ho Yin Edwin Chan[1,2,3,4,*]

[1]Laboratory of Drosophila Research, [2]Cell and Molecular Biology Program, [3]Molecular Biotechnology Program and [4]Department of Biochemistry, Faculty of Science, The Chinese University of Hong Kong, Shatin, N.T., Hong Kong SAR, China, [5]Division of Molecular and Cell Biology, School of Biological Sciences, College of Science, Nanyang Technological University, 637551 Singapore and [6]Department of Genetics and Howard Hughes Medical Institute, Harvard Medical School, Boston, MA 02115, USA

Received December 25, 2010; Revised December 25, 2010; Accepted February 2, 2011

Polyglutamine (polyQ) diseases are a group of late-onset, progressive neurodegenerative disorders caused by CAG trinucleotide repeat expansion in the coding region of disease genes. The cell nucleus is an important site of pathology in polyQ diseases, and transcriptional dysregulation is one of the pathologic hallmarks observed. In this study, we showed that exportin-1 (Xpo1) regulates the nucleocytoplasmic distribution of expanded polyQ protein. We found that expanded polyQ protein, but not its unexpanded form, possesses nuclear export activity and interacts with Xpo1. Genetic manipulation of *Xpo1* expression levels in transgenic *Drosophila* models of polyQ disease confirmed the specific nuclear export role of Xpo1 on expanded polyQ protein. Upon *Xpo1* knockdown, the expanded polyQ protein was retained in the nucleus. The nuclear disease protein enhanced polyQ toxicity by binding to *heat shock protein (hsp)* gene promoter and abolished *hsp* gene induction. Further, we uncovered a developmental decline of Xpo1 protein levels *in vivo* that contributes to the accumulation of expanded polyQ protein in the nucleus of symptomatic polyQ transgenic mice. Taken together, we first showed that Xpo1 is a nuclear export receptor for expanded polyQ domain, and our findings establish a direct link between protein nuclear export and the progressive nature of polyQ neurodegeneration.

INTRODUCTION

Polyglutamine (polyQ) diseases are a group of neurodegenerative disorders characterized by the pathogenic expansion of existing CAG trinucleotide repeats in the coding region of disease genes, which are translated into expanded polyQ domains in disease proteins (1). Despite the diverse regional vulnerabilities of the nine polyQ diseases identified thus far, they share several salient pathologic features, including progressive neurodegeneration usually striking in midlife, formation of insoluble protein aggregates and transcriptional dysregulation of essential genes in affected neurons (1). The cell nucleus is regarded as a major site of toxicity in different polyQ disease models (2–11). The nucleocytoplasmic localization of cellular proteins is governed by nuclear transport signals, which are short stretches of amino acids on them and recognized by specific transport receptors/adaptors (12). The nuclear transport receptors/adaptors interact with their

*To whom correspondence should be addressed. Tel: +852 3163 4021; Fax: +852 2603 7732; Email: hyechan@cuhk.edu.hk
†These authors contributed equally to this work.

substrates and mediate nuclear transport across the nuclear envelope (13). Previous studies show that polyQ domain expansion not only causes nuclear localization of disease protein (14), but also compromises the function of nuclear transport signals on disease proteins and thus alters their subcellular localization (15,16).

To investigate the nuclear transport property of expanded polyQ domain *per se*, we initially took advantage of an inducible *Drosophila* cell model to test whether any nuclear transport receptors/adaptors would modulate expanded polyQ protein nucleocytoplasmic localization. Notably, our knockdown data implied that expanded polyQ domain mediated protein nuclear export through an exportin-1 (Xpo1)-dependent pathway. We then focused on elucidating the nuclear export property of an expanded polyQ domain and its associated modification on polyQ toxicity by Xpo1. We found that an expanded polyQ domain, but not its unexpanded form, carried nuclear export activity and physically interacted with Xpo1. Retention of expanded polyQ protein in the nucleus due to *Xpo1* knockdown led to impairment of *heat shock protein* (*hsp*) gene induction and therefore enhanced toxicity. This suggests that nuclear export of expanded polyQ protein helps in maintaining the cellular heat shock response during the course of polyQ pathogenesis. We also reported a temporal decline of Xpo1 levels in both wild-type and polyQ transgenic mice. The gradual decrease of Xpo1 protein levels during aging explains, at least in part, the progressive nature of polyQ neurodegeneration. This study first reports an expanded polyQ domain-specific nuclear export pathway, which involves Xpo1 as the export receptor. Identifying the nuclear transport pathways that govern the nucleocytoplasmic localization of expanded polyQ protein will open up new directions for mechanistic studies of polyQ pathogenesis and therapeutic development.

RESULTS

Nuclear transport receptors/adaptors modulate subcellular localization of polyQ aggregates

An inducible *Drosophila* neuronal BG2 cell model that stably expressed enhanced green fluorescent protein (EGFP)–polyQ fusion proteins (EGFP–Q27 or EGFP–Q75) was established to study the nuclear transport property of polyQ domain. At 96 h post-induction, the unexpanded EGFP–Q27 was found diffusely localized in both the cytoplasm and nucleus of BG2 cells, whereas expanded EGFP–Q75 formed aggregates in both compartments (Fig. 1A). In order to test whether nuclear transport receptor/adaptor would regulate the nucleocytoplasmic distribution of proteins carrying an expanded polyQ domain, the expression of 19 *receptor/adaptor* genes in the *Drosophila* genome was knocked down by double-stranded RNA (dsRNA) in BG2 cells (Fig. 1B), and their effects on the subcellular localization of expanded polyQ protein were examined (Table 1). Among all the genes investigated, *Xpo1* was the only one whose knockdown caused a significant buildup of EGFP–Q75 in the nucleus. No such effect was observed with the unexpanded EGFP–Q27 control (data not shown), implying the *Xpo1* knockdown effect is expanded polyQ specific.

Expanded polyQ domain mediates protein nuclear export through an Xpo1-dependent pathway

Exportin-1 is a well-characterized nuclear export receptor (17). Our *Xpo1* knockdown data (Table 1) advocated the claim that the expanded polyQ protein is an export substrate of Xpo1. We therefore sought to assess the nuclear export activity of expanded polyQ domain by the well-established Rev(1.4)–EGFP nuclear export assay (18). To do this, different lengths of polyQ domains were tagged to the Rev(1.4)–EGFP reporter protein (Supplementary Material, Fig. S1A). Transfected HEK293 cells were treated with cycloheximide and actinomycin D to stop protein synthesis and nuclear import of the Rev(1.4)–polyQ–EGFP reporter protein, respectively (18). Any green fluorescent protein (GFP) signal detected in the cytoplasm would thus be attributable to the nuclear export activity conferred by the appended polyQ domain. The controls, i.e. Rev(1.4)–EGFP protein carrying either no (Q0) or an unexpanded (Q19) polyQ domain, showed a predominant nuclear localization (Fig. 2A and B), indicating that unexpanded polyQ domain has no detectable nuclear export signal (NES) activity. However, the addition of an expanded polyQ domain (Q78) to Rev(1.4)–EGFP caused a significant cytoplasmic shift of the reporter protein (Fig. 2A and B). This clearly demonstrated that expanded polyQ domain possesses nuclear export activity. To confirm the involvement of Xpo1 in mediating the nuclear export of expanded polyQ domain-containing protein, we treated cells with leptomycin B (LMB), a potent inhibitor of Xpo1-mediated nuclear export (19,20). Upon LMB treatment, we found a noticeable nuclear shift of Rev(1.4)–Q78–EGFP from the cytoplasm (Fig. 2A). Consistent with western blot analysis (Fig. 2A), we observed a significant reduction in the number of cells that displayed cytoplasmic localization of the Rev(1.4)–Q78–EGFP protein after LMB treatment (Fig. 2B). We also observed a similar change in Rev(1.4)–Q78–EGFP subcellular localization when *Xpo1* expression was knocked down by small interfering RNA (siRNA) in HEK293 cells (Fig. 2C and D; Supplementary Material, Fig. S1B). Altogether, our data clearly demonstrated that expanded polyQ domain is a functional NES and Xpo1 is the receptor that mediates protein nuclear export of expanded polyQ protein.

To gain further insight into the involvement of Xpo1 in expanded polyQ domain-mediated nuclear export, we tested whether an expanded polyQ domain would physically interact with Xpo1. By using a series of myc-tagged polyQ–EGFP fusion constructs (21), we showed that Xpo1 interacted only with Q81–EGFP, but not with Q19–EGFP, in HEK293 cells (Fig. 3A). Similar expanded polyQ-specific interactions were also observed between Xpo1 and disease proteins, including those that cause Machado Joseph Disease [Machado-Joseph Disease (MJD); MJDtrQ78; Fig. 3B] and Huntington's disease (HD; Htt_{1-550}Q83; Fig. 3C). Notably, we found that Xpo1 interacted only with sodium dodecylsulphate (SDS)-soluble Q81-EGFP, but not with the SDS-insoluble ones resided in stacking gel (Supplementary Material, Fig. S2). This indicates that such protein–protein interaction is not mediated through non-specific recruitment to protein aggregates. As the interaction between Xpo1 and its export substrate is a pre-requisite for receptor-mediated protein nuclear export

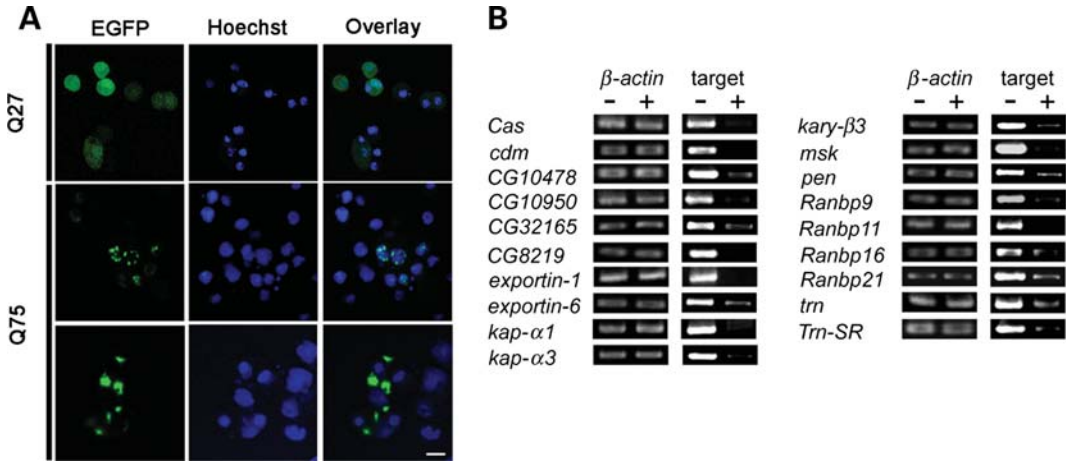

Figure 1. Subcellular localization of EGFP–Q75 aggregates in *Drosophila* neuronal BG2 cells. (**A**) At 96 h post-induction, EGFP–Q27 localized homogeneously in BG2 cells, while EGFP-Q75 formed aggregates in both cytoplasm and nucleus. Scale bar represents 5 μm. (**B**) The knockdown efficiency of dsRNAs used in this study. Compared with water-treated control (−), treatment of BG2 cells with specific dsRNAs (+) caused a reduction in target gene mRNA. *β-actin* was used as a loading control.

Table 1. Gene knockdown effects of different nuclear transport receptors/adaptors on the subcellular localization of EGFP-Q75 in *Drosophila* neuronal BG2 cells

Gene	Average no. of cells with NAs	Average no. of cells with CAs	Average no. of cells with NAs and CAs
–	33 ± 5	44 ± 1	23 ± 6
Cas	33 ± 3	48 ± 2	19 ± 5
cdm	25 ± 4	55 ± 2	20 ± 4
CG10478	34 ± 6	48 ± 4	18 ± 2
CG10950	37 ± 2	47 ± 4	16 ± 7
CG32165	37 ± 3	47 ± 5	16 ± 6
CG8219	34 ± 3	52 ± 4	14 ± 1
Exportin-1	59 ± 1	30 ± 3	11 ± 2
Exportin-6	32 ± 6	50 ± 3	18 ± 3
Kap-α1	26 ± 3	56 ± 3	18 ± 1
Kap-α3	24 ± 3	56 ± 4	20 ± 5
Kary-β3	26 ± 4	54 ± 5	20 ± 1
msk	40 ± 1	44 ± 5	16 ± 6
pen	31 ± 2	50 ± 10	19 ± 7
Ranbp9	36 ± 3	46 ± 4	18 ± 5
Ranbp11	35 ± 2	47 ± 6	18 ± 3
Ranbp16	35 ± 3	49 ± 2	16 ± 2
Ranbp21	34 ± 3	46 ± 3	20 ± 1
trn	34 ± 4	49 ± 2	17 ± 6
Trn-SR	37 ± 7	47 ± 2	16 ± 5

One hundred cells were counted in each experiment, and a total of 300 cells were counted from three independent experiments (mean ± SD). CA and NA denote cytoplasmic and nuclear aggregates, respectively. '–' represents no dsRNA control.

(17), we demonstrated here that the pathogenic expansion of polyQ domain renders disease protein an ability to interact with Xpo1 and hence mediates its nuclear export.

Expanded polyQ protein/Xpo1 interaction does not affect cellular Xpo1-mediated protein nuclear export

We next addressed whether the interaction between expanded polyQ protein and Xpo1 would lead to the sequestration of Xpo1 into protein aggregates, like the cAMP response element-binding protein (22), and hence perturb its normal function. We found that Xpo1 was not recruited to polyQ aggregates, endogenous Xpo1 appeared in the same diffuse pattern in both Q19– and Q81–EGFP-expressing cells (Fig. 4A). This result implied that the endogenous function of Xpo1 was not affected by its interaction with soluble expanded polyQ protein. Further, we found that the Xpo1 nuclear export machinery remained intact (Fig. 4B and C). Survivin, an endogenous export substrate of Xpo1, normally localizes predominantly to the cytoplasm (23). We observed a cytoplasmic localization of survivin in HEK 293 cells expressing either Q19- or Q81-EGFP (Fig. 4B). Exportin-1 forms high-molecular-weight protein complexes with its substrates (17). Similar to the Q19–EGFP control, we also observed high-molecular-weight Xpo1 protein complex formation in Q81–EGFP-expressing cells (Fig. 4C). In line with the above findings, we also detected an intact Ran gradient across the nuclear envelope in Q81–EGFP-expressing cells (Supplementary Material, Fig. S3), which is essential for Xpo1-mediated protein nuclear export (17). Altogether, our data showed that the expression of expanded polyQ protein does not abolish the export role of Xpo1 for other cellular proteins.

Exportin-1 modulates polyQ toxicity by altering nucleocytoplasmic localization of expanded polyQ proteins

In an attempt to correlate the nuclear export activity of expanded polyQ domain to polyQ toxicity, we further extended our study to *in vivo* transgenic disease models. The full-length *MJD* transgene, *MJDQ84*, was expressed in adult *Drosophila* retinal neurons using the GAL4/UAS system (Fig. 5). Neurotoxicity of this model has previously been described (24). When *Xpo1* expression was knocked down by dsRNA (Supplementary Material, Fig. S4), its nuclear export substrate, MJDQ84, retained predominantly in the nucleus (Fig. 5A and B). In contrast, *Xpo1* over-expression (Supplementary Material, Fig. S4) promoted MJDQ84 nuclear export and thus resulted in a cytoplasmic enrichment of MJDQ84 (Fig. 5A and B). Consistent with our *in vitro* binding data that only the expanded polyQ

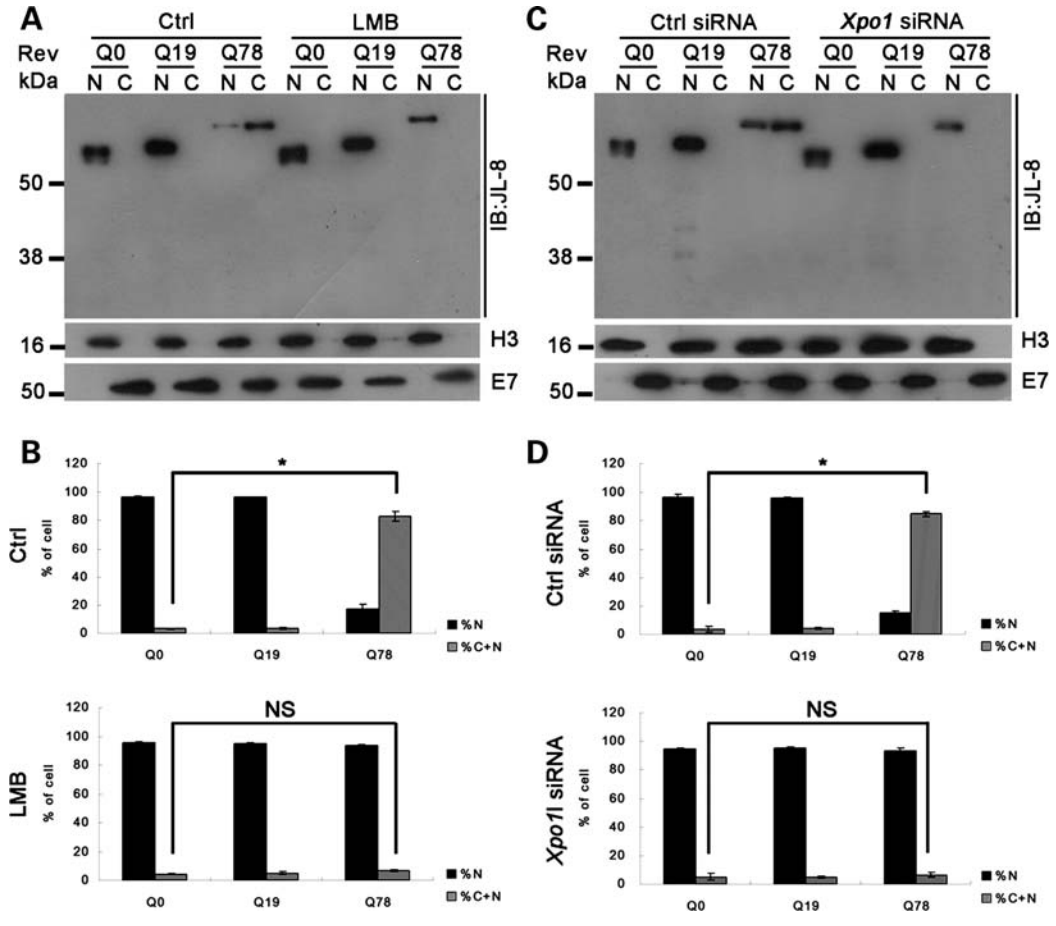

Figure 2. Expanded polyQ domain shows nuclear export activity. (**A** and **C**) Nucleocytoplasmic fractionation of Rev(1.4)–polyQ–EGFP reporter proteins in HEK293 cells. Both Rev(1.4)–Q0–EGFP and Rev(1.4)–Q19–EGFP proteins were predominantly found in the nucleus. In contrast, majority of the Rev(1.4)–Q78–EGFP protein was detected in the cytoplasmic fraction ($n = 3$). (A) Upon LMB treatment, cytoplasmic Rev(1.4)–Q78–EGFP was re-distributed to the nuclear fraction. A similar effect was observed on Rev(1.4)–Q78–EGFP when *Xpo1* expression was knocked down by siRNA (C). Anti-GFP antibody JL-8 was used to detect the Rev(1.4)–polyQ–EGFP proteins. The same blot was stripped and re-probed with anti-β-tubulin E7 and anti-histone H3 antibodies. (**B** and **D**) The Rev(1.4) nuclear export assay ($^*P < 0.005$, $n = 5$; NS denotes not statistically significant). Both Rev(1.4)–Q0–EGFP and Rev(1.4)–Q19–EGFP protein displayed no nuclear export activity, and localized predominantly to the nucleus. The addition of an expanded polyQ domain (Q78) to Rev(1.4)–EGFP caused an increase in number of cells displayed cytoplasmic (C + N) localization. Upon LMB treatment, the number of cells with C + N localization returned back to the Rev(1.4)–Q0/Q19–EGFP control level (B). A similar effect on the Rev(1.4)–Q78–EGFP protein was also observed when *Xpo1* expression was knocked down by siRNA (D). Rev, Rev(1.4)–EGFP; N, nuclear; C, cytoplasmic; C + N, cytoplasmic and nuclear.

proteins interacts with Xpo1 (Fig. 3 and Supplementary Material, Fig. S2), the unexpanded control (MJDQ27) did not show such modulation of its subcellular localization upon *Xpo1* knockdown (Fig. 5A). This clearly demonstrated that Xpo1 specifically modifies the subcellular localization of expanded polyQ protein. As the depletion of Xpo1 enhanced retinal degeneration while its overexpression attenuated MJDQ84 toxicity (Fig. 5C and D; 25), our data indicated that the subcellular localization of MJDQ84 is tightly linked to degeneration and that MJDQ84 exerts its toxicity predominantly in the nucleus.

The modifying effect of *Xpo1* was also tested in other *Drosophila* models of neurodegenerative diseases, including more polyQ diseases and Parkinson's disease. Among all the polyQ disease models investigated, including those for spinal and bulbar muscular atrophy (26), HD (27) and an artificial EGFP–Q76 model (28), the knockdown of *Xpo1* expression all enhanced polyQ toxicity (Supplementary Material, Fig. S5). In contrast, the neurotoxicity caused by α-synuclein (the disease protein for Parkinson's disease) (29) was insensitive to Xpo1 (Supplementary Material, Fig. S6). Therefore, our results support the notion that Xpo1 specifically modulates expanded polyQ-induced toxicity.

Nuclear disease protein enhances polyQ toxicity by suppressing the cellular heat shock response

We then investigated how nuclear accumulation of MJDQ84 caused polyQ toxicity. Heat shock response is a cellular defense mechanism to prevent misfolding and/or aggregation of disease proteins (30). The expression of expanded polyQ protein elicits heat shock response through the induction of *hsp* gene expression. However, we have previously reported that the continuous expression of the expanded truncated MJD protein (MJDtrQ78) *in vivo* would cause a reduction in *hsp* gene induction (31). Such biphasic *hsp* gene expression

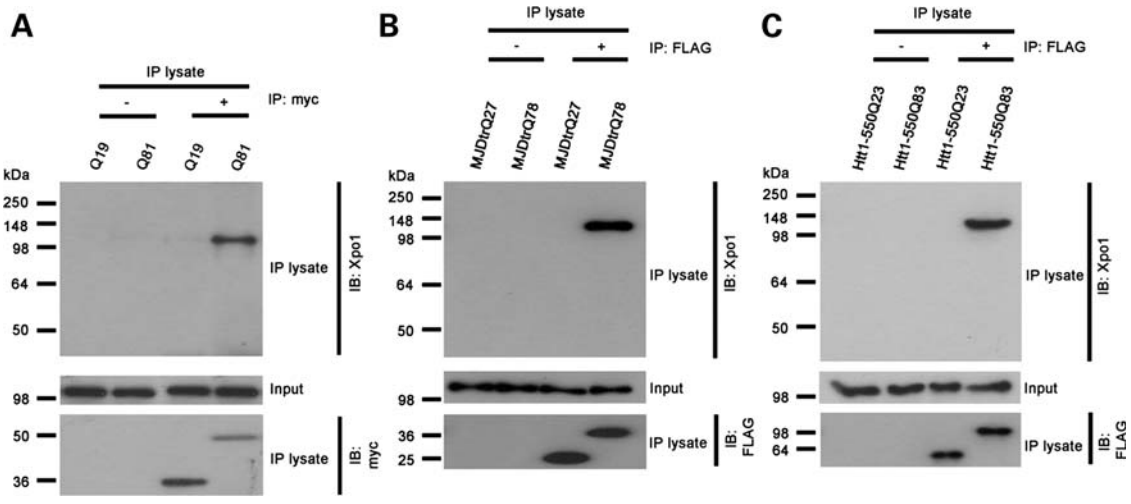

Figure 3. Expanded polyQ proteins interact with Xpo1. (**A**) The myc-tagged expanded polyQ domain-containing protein Q81–EGFP, but not the unexpanded Q19–EGFP control, interacted with Xpo1. (**B** and **C**) Similarly, only the polyQ domain-expanded FLAG-tagged polyQ disease proteins, MJDtrQ78 (B) and $Htt_{1-550}Q83$ (C), interacted with Xpo1.

profile has also been reported in different polyQ disease models (31–33). As reported earlier (31), we also detected an induction of *hsp70* mRNA expression in this full-length MJDQ84 transgenic fly model (Fig. 6A, lane 8). Similar induction of other *hsps*, including *hsp22* and *hsp40*, was also observed (data not shown). Nonetheless, such induction was diminished in MJDQ84 flies co-expressing *Xpo1* dsRNA (Fig. 6A, lane 9). We further showed that the general *hsp* gene induction machinery in *MJDQ84/ds_Xpo1* double-transgenic flies was compromised as they failed to respond to elevated temperature, a universal heat shock stimulus (Fig. 6A, lane 9). Interestingly, the expression of MJDQ84 protein alone did not cause any defect in general heat shock response (Fig. 6A, lane 8), so as when *Xpo1* expression was knocked down alone (Fig. 6A, lane 3) or in *MJDQ27/ds_Xpo1* double-transgenic flies (Fig. 6A, lane 6). The above observations clearly indicated that the absence of *hsp70* induction in the *MJDQ84/ds_Xpo1* double-transgenic flies (Fig. 6A, lane 9) was not simply a consequence of *Xpo1* knockdown, but an effect in association with the expression of MJDQ84. We further demonstrated that the overexpression of *Xpo1* in MJDQ84 flies could robustly induce (Fig. 6, lane 10) and prolong (Supplementary Material, Fig. S7) *hsp70* expression. As Hsp70 has been reported to play neuroprotective roles in polyQ degeneration (30), our findings reinforced the idea that strategies that can maintain *hsp* gene induction are beneficial to polyQ degeneration.

It has previously been reported that expanded polyQ disease proteins can bind to gene promoters (34). By performing chromatin immunoprecipitation, we demonstrated an interaction between expanded polyQ protein and *hsp70* promoter (Fig. 6B and Supplementary Material, Fig. S8). Further, we found that *Xpo1* knockdown promoted the MJDQ84/*hsp70* promoter protein–DNA interaction, whereas overexpression of *Xpo1* reduced such binding (Fig. 6C). The enhancement effect of MJDQ84 degeneration caused by *Xpo1* knockdown (Fig. 5C and D) could therefore be explained by the impairment of MJDQ84 protein nuclear export, which then promoted the binding of MJDQ84 onto the *hsp70* promoter and subsequently caused a blockade of *hsp70* gene induction. When we bypassed the endogenous cellular heat shock gene induction mechanism and overexpressed a human *hsp70* transgene *HSPA1L* (35) in *MJDQ84/ds_Xpo1* double-transgenic flies via the GAL4/UAS transgene expression system, MJDQ84 degeneration was almost completely suppressed (Fig. 6D and E). In addition, we showed that Xpo1 does not exert the same effect on α-synuclein ((36); Fig. 6A, lanes 11–13). First, we did not observe *hsp70* gene induction in the α-synuclein model (Fig. 6A, lane 11). Secondly, the knockdown of *Xpo1* expression in α-synuclein flies did not cause any impairment of the general heat shock response (Fig. 6A, lane 12). We therefore confirmed that *Xpo1* knockdown specifically intensifies MJDQ84 neurodegeneration through blockade of cellular heat shock response.

The decline of Xpo1 protein level with age explains the progressive nature of polyQ disease

Transcriptional dysregulation is one of the pathogenic hallmarks of polyQ diseases (1). We found that the enhancing effect of *Xpo1* knockdown on expanded polyQ-induced degenerative phenotype (Fig. 5C and D) was accompanied by a reduction in *hsp* gene induction (Fig. 6). The late-onset and progressive nature of polyQ diseases prompted us to determine the temporal expression level of Xpo1 in an organism. Interestingly, we observed a temporal decline of the Xpo1 protein levels in both the R6/2 HD transgenic mice (37,38) (Fig. 7A and B) and wild-type mice (Supplementary Material, Fig. S9). This clearly showed a gradual reduction in the Xpo1 protein levels with time. In relation to this, we also detected a concomitant age-dependent accumulation of expanded Htt protein in the nuclear fraction isolated from symptomatic R6/2 mice (Fig. 7C). Taken together, our R6/2 biochemical analyses (Fig. 7) are in good agreement with the *Xpo1* knockdown data that observed in the fly studies (Fig. 5). This indicated that the developmental decline of the Xpo1 protein

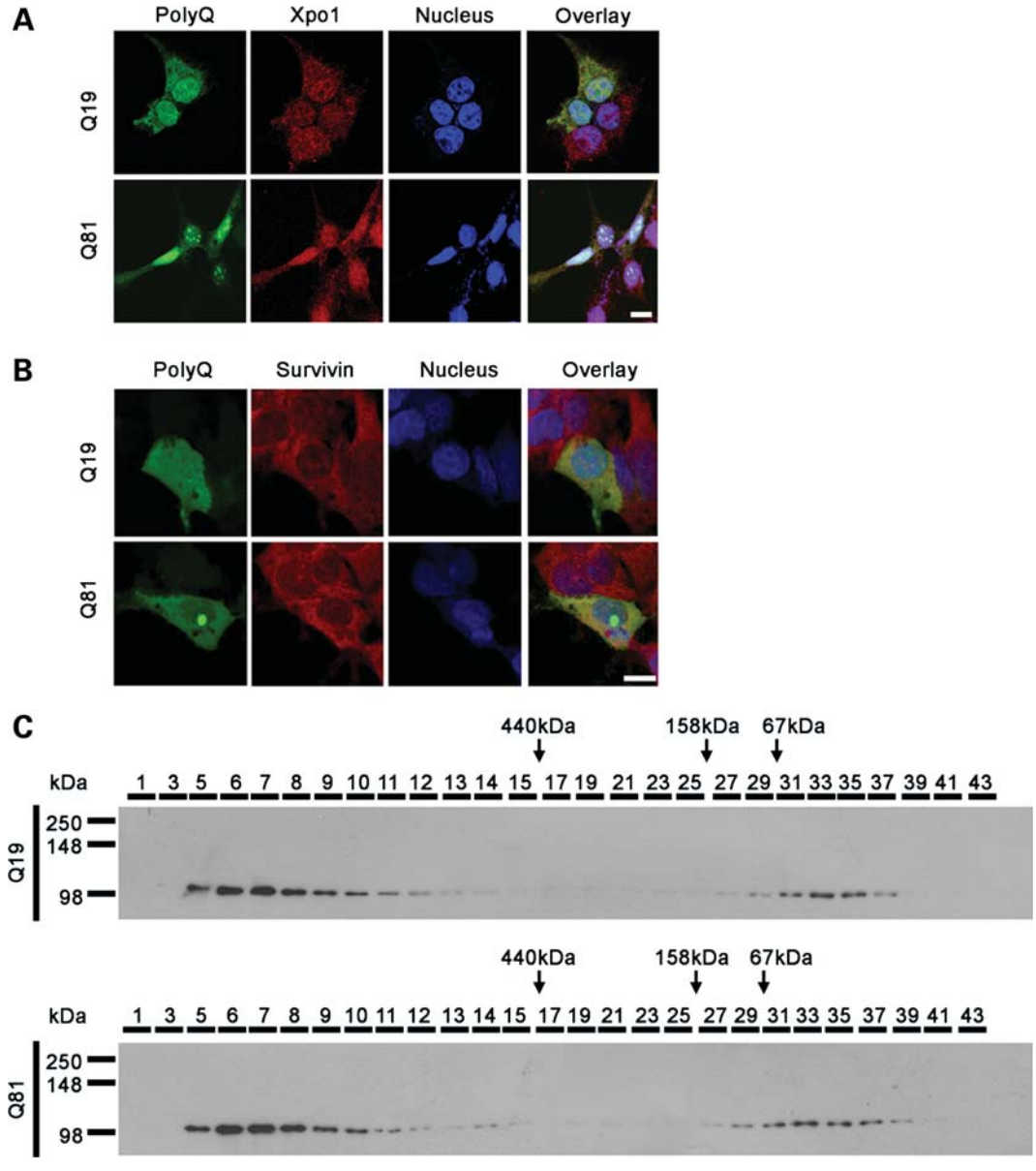

Figure 4. The protein nuclear export machinery of Xpo1 remains functional in expanded polyQ protein-expressing cells. (**A**) HEK293 cells transfected with Q19/Q81–EGFP were stained with anti-Xpo1 antibody. Both Q19– and Q81–EGFP proteins were found to be present in both nucleus and cytoplasm. Diffuse Xpo1 staining signal was detected mainly in the nucleus in both Q19– and Q81–EGFP-expressing cells. The Q81–EGFP protein formed protein aggregates in the nucleus, but Xpo1 was not recruited to the aggregates. Scale bar represents 20 μm. (**B**) Transfected HEK293 cells were stained with anti-survivin antibody. Survivin localized predominantly to the cytoplasm in both Q19– and Q81–EGFP-expressing cells. Scale bar represents 20 μm. (**C**) Total HEK293 cell lysates were harvested and subjected to size exclusion chromatography. High-molecular-weight complexes containing Xpo1 (fractions 5–10) were observed in both Q19– and Q81–EGFP lysates, indicating that the interaction between Xpo1 and Q81-EGFP does not disrupt Xpo1 protein complex formation.

levels contributes to the progressive buildup of expanded polyQ protein in the nucleus and hence promotes toxicity.

DISCUSSION

The nucleocytoplasmic localization of expanded polyQ proteins plays a pivotal role in the degenerative process of polyQ diseases (39). Although nuclear transport signals have been identified in non-polyQ regions of different disease proteins (3–5,16,40–47), proteolytic cleavage is commonly observed and generates truncated polyQ domain-containing disease proteins that lack these signals (48). Therefore, the polyQ domain itself is believed to play a determining role in the subcellular localization of disease proteins. In view of this, we used an EGFP–polyQ reporter to investigate the nuclear transport property of expanded polyQ domain. From our knockdown study carried out in BG2 cells, we identified several nuclear transport receptors/adaptors whose depletion caused altered subcellular localization of expanded polyQ protein (Fig. 1 and Table 1). Pathogenic expansion of polyQ domain has previously been shown to dictate nuclear

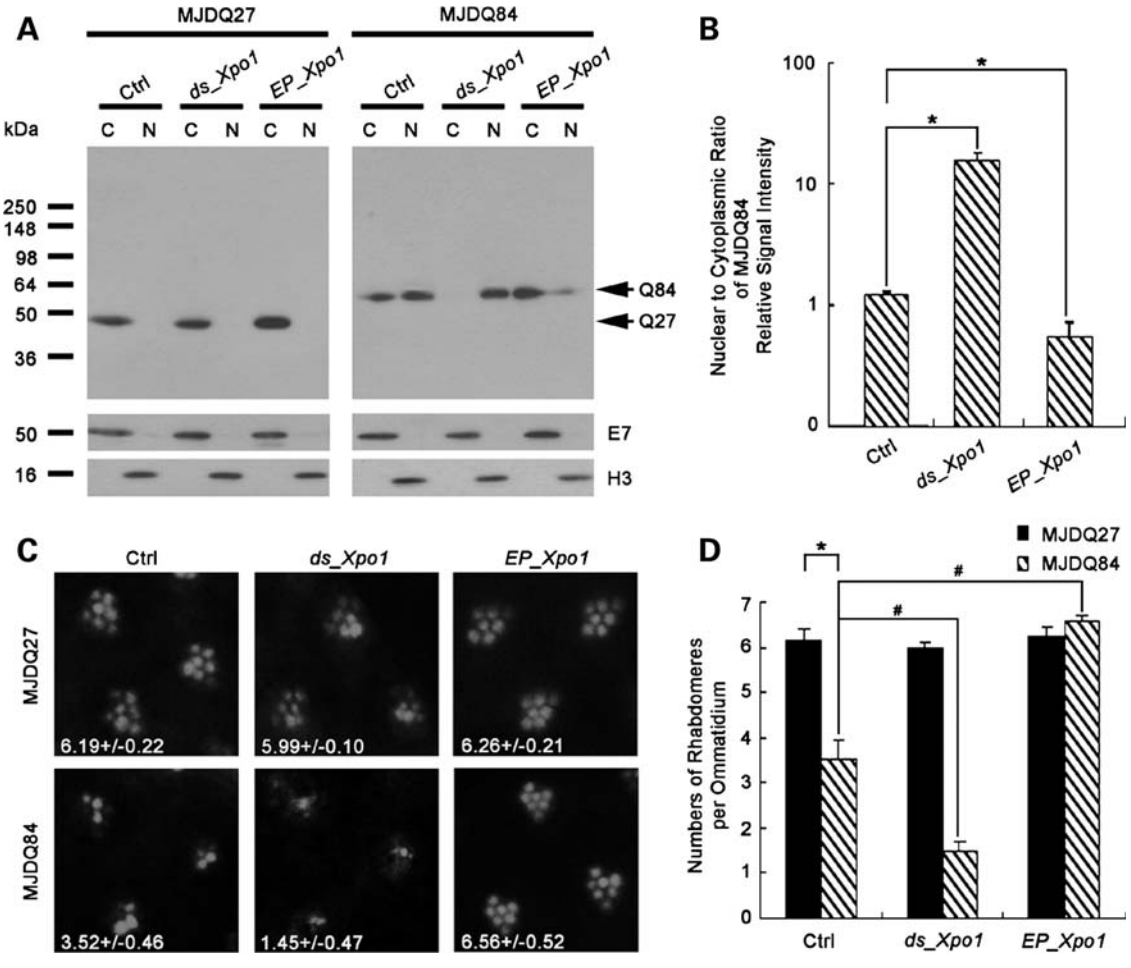

Figure 5. Modulation of polyQ toxicity by Xpo1 is accompanied by an alteration of expanded polyQ protein nucleocytoplasmic localization. (**A**) Western blot analysis of formic acid-treated cytoplasmic (C) and nuclear (N) myc-tagged full-length MJD proteins isolated from 0- to 2-day-old flies. By using the anti-myc antibody, the unexpanded MJDQ27 protein was detected exclusively in the cytoplasmic fraction, while the expanded MJDQ84 protein was detected in both the cytoplasmic and nuclear fractions. The same blot was stripped and re-probed with anti-β-tubulin E7 and anti-histone H3 antibodies. (**B**) Densitometric analysis of (A). *Exportin-1* knockdown caused nuclear retention of MJDQ84 whereas its overexpression resulted in predominant cytoplasmic localization of MJDQ84. The data are presented as the band intensity ratio of nuclear to cytoplasmic (N/C) MJD protein (mean + SEM, $^{*}P < 0.05$, $n = 4$). (**C**) Representative images of rhabdomeres taken from 0- to 2-day-old adult flies. (**D**) Quantification of (C). Expression of MJDQ84 alone caused a significant reduction in the number of rhabdomeres ($^{*}P < 0.001$, $n = 3$). Either the knockdown or over-expression of *Xpo1* resulted in a significant change in the number of rhabdomeres ($^{\#}P < 0.001$, $n = 3$). Error bars represent SEM. The flies were of genotypes *w; gmr-GAL4 UAS-myc-MJDQ27/+, w; gmr-GAL4 UAS-myc-MJDQ27/UAS-Xpo1-dsRNA, w; gmr-GAL4 UAS-myc-MJDQ27/Xpo1$^{EP\text{-}E128\text{-}1A}$, w; gmr-GAL4/+; UAS-myc-MJDQ84/+, w; gmr-GAL4/UAS-Xpo1-dsRNA; UAS-myc-MJDQ84/+, and w; gmr-GAL4/Xpo1$^{EP\text{-}E128\text{-}1A}$; UAS-myc-MJDQ84/+*.

localization of a cytoplasmic protein (14), yet the detailed import machinery remained mysterious.

In this study, we reported, for the first time, that expanded polyQ domain possesses NES activity. Consistent with this view, it has previously been reported that the disease protein for dentatorubral and pallidoluysian atrophy, Atrophin-1, when carrying an expanded polyQ domain was found to localize more frequently to the cytoplasm when compared with its unexpanded form (5). Exportin-1 is the nuclear export receptor for the classical leucine-rich NESs (17). LMB covalently modifies the Cys-529 residue in the NES-binding pocket of Xpo1 which subsequently causes inactivation of Xpo1's nuclear export activity (49). Although expanded polyQ domain shows no resemblance to this group of NES, our LMB treatment and knockdown results clearly demonstrate that Xpo1 mediates its nuclear export (Figs 1–3). Both our *in vitro* (Figs 1 and 2) and *in vivo* (Fig. 5A and B) data showed that the knockdown of *Xpo1* expression leads to nuclear accumulation of expanded polyQ protein but exerts no modulatory effect on the unexpanded protein. Together with the demonstrated interaction between expanded polyQ domain and Xpo1 (Fig. 3A and Supplementary Material, Fig. S2), we believe that the pathogenic expansion of polyQ domain directs the disease protein to adopt an aberrant conformation that is able to be recognized by Xpo1. As Xpo1 interacts only with SDS-soluble Q81–EGFP (Supplementary Material, Fig. S2) and is not sequestered to polyQ protein aggregates (Fig. 4A), such interaction *per se* does not impose any adverse effect to the cellular Xpo1-mediated nuclear export machinery (Fig. 4B and C).

Being an Xpo1 export substrate (Fig. 2), majority of cells we analyzed showed diffuse cytoplasmic Q81–EGFP

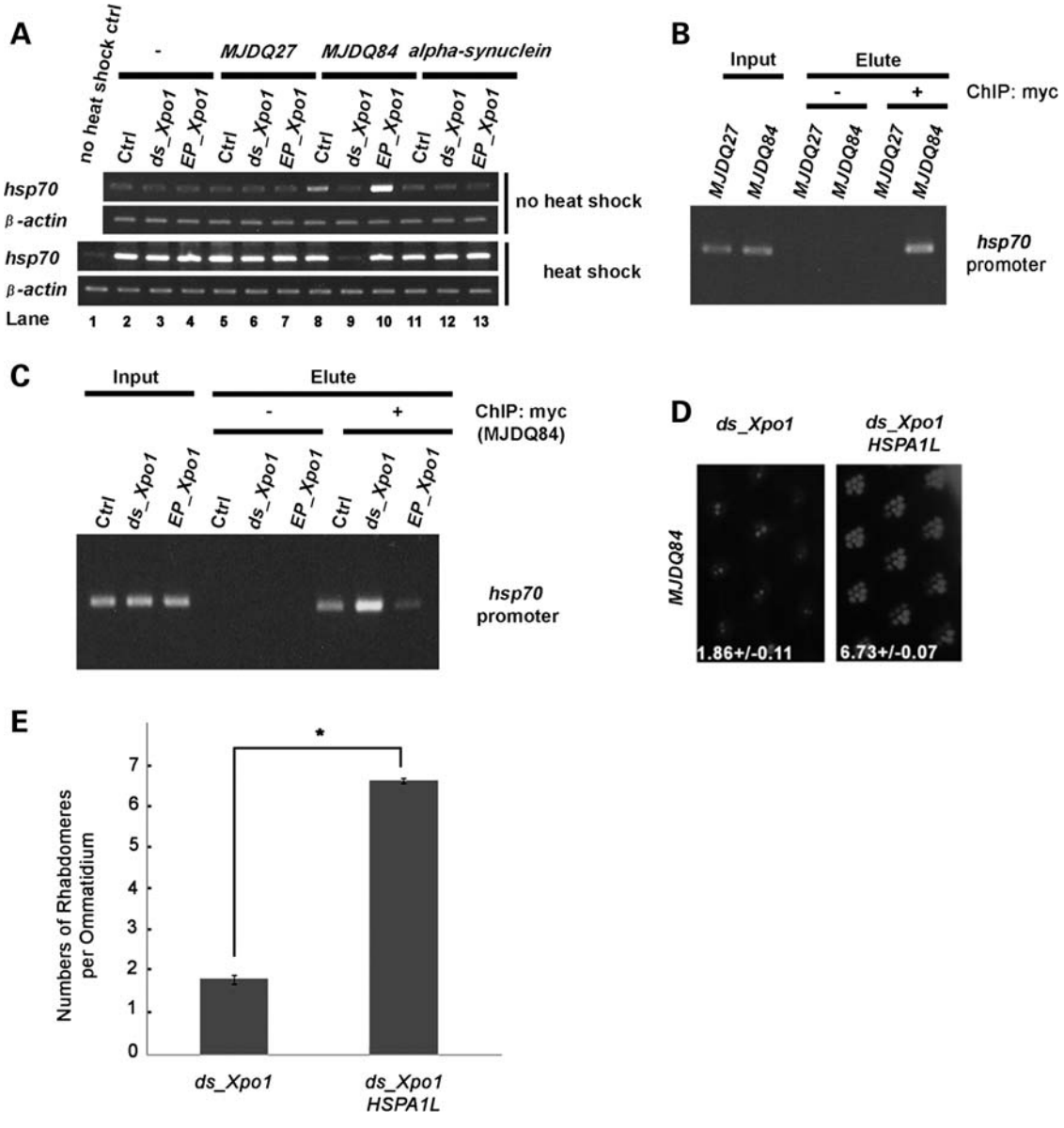

Figure 6. The nuclear MJDQ84 protein causes toxicity by suppressing cellular heat shock response. (**A**) Heat shock response in polyQ flies expressing different levels of *Xpo1*. Expression of full-length MJD unexpanded polyQ protein MJDQ27 (lane 5) did not cause *heat shock* gene induction, as *hsp70* expression in MJDQ27 flies remained at the non-transgenic control level (lane 2). In contrast, expression of expanded MJDQ84 protein in flies induced *hsp70* expression (lane 8). Knockdown of *Xpo1* expression (Supplementary Material, Fig. S4) in MJDQ84 flies (lane 9) impaired *hsp70* induction. In contrast, overexpression of *Xpo1* (Supplementary Material, Fig. S4) promoted *hsp70* induction (lane 10). Modulation of *Xpo1* expression levels in the presence (lanes 6 and 7) or absence (lanes 3 and 4) of MJDQ27 expression in flies did not alter *hsp70* expression level. The *hsp70* level remained unchanged in α-synuclein flies expressing either normal endogenous (lane 11), reduced (lane 12) or overexpressed (lane 13) levels of *Xpo1*. Compared with the untreated (no heat shock) control (lane 1), heat shock treatment led to robust *hsp70* induction in all samples except for flies co-expressing MJDQ84 and *Xpo1 dsRNA* (lane 9). *β-actin* was used as a loading control. The experiment has been repeated for three times. '–' denotes no transgene expression control. (**B**) Expanded polyQ protein MJDQ84 interacted with the *hsp70* promoter *in vivo* ($n = 3$). (**C**) When compared with flies expressing MJDQ84 alone, MJDQ84 flies co-expressing *Xpo1 dsRNA* and *Xpo1* transgene, respectively, promoted and reduced MJDQ84/*hsp70* promoter protein–DNA interaction ($n = 3$). (**D**) Expression of human *hsp70*, *HSPA1L*, via the GAL4/UAS transgenic overexpression system rescued degeneration caused by MJDQ84/*Xpo1 dsRNA* coexpression. (**E**) Quantification of (D) ($^*P < 0.001$, $n = 3$). The flies were of genotypes *w; gmr-GAL4/+, w; gmr-GAL4 UAS-myc-MJDQ27/+, w; gmr-GAL4 UAS-myc-MJDQ27/UAS-Xpo1-dsRNA, w; gmr-GAL4 UAS-myc-MJDQ27/Xpo1*$^{EP\text{-}E128\text{-}1A}$, *w; gmr-GAL4/+; UAS-myc-MJDQ84/+, w; gmr-GAL4/UAS-Xpo1-dsRNA; UAS-myc-MJDQ84/+, w; gmr-GAL4/Xpo1*$^{EP\text{-}E128\text{-}1A}$*; UAS-myc-MJDQ84/+, w; gmr-GAL4/+; UAS-α-synuclein*^{wt}*/+, w; gmr-GAL4/UAS-Xpo1-dsRNA; UAS-α-synuclein*^{wt}*/+, w; gmr-GAL4/Xpo1*$^{EP\text{-}E128\text{-}1A}$*; UAS-α-synuclein*^{wt}*/+* and *w; gmr-GAL4 UAS-Xpo1-dsRNA/UAS-HSPA1L; UAS-myc-MJDQ84/+*.

localization (Table 2). However, we also found cells that only showed nuclear Q81–EGFP signals (Fig. 4A and Table 2). We believe that these signals would be contributed by the SDS-insoluble Q81–EGFP protein species resided in the nucleus. Since we demonstrated that SDS-insoluble polyQ protein is incapable of interacting with Xpo1 (Supplementary Material, Fig. S2), protein of such property would not be able to be exported out of the nucleus and thus become

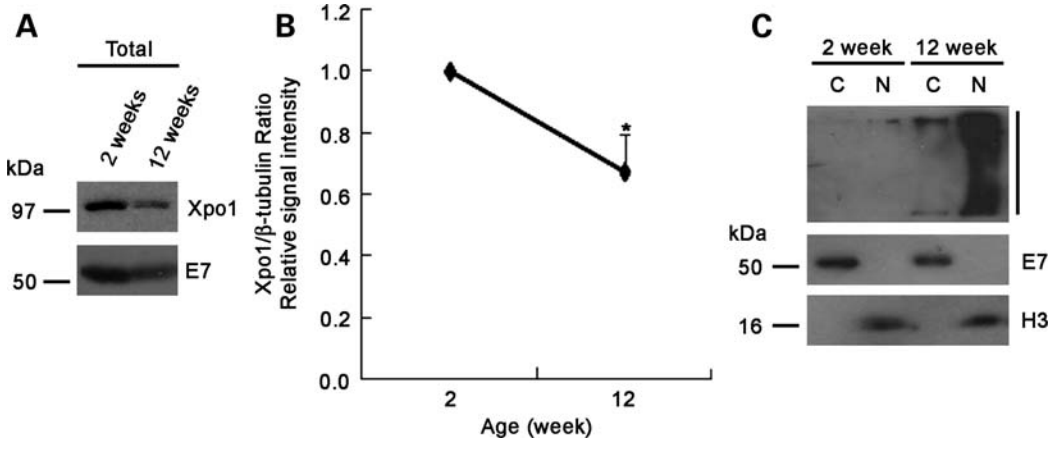

Figure 7. Exportin-1 protein level diminishes with time and such decline is accompanied by nuclear accumulation of SDS-insoluble expanded Huntingtin protein in R6/2 HD transgenic mice. (**A**) A representative western blot of the detection of Xpo1 protein in whole brain lysates using anti-Htt antibody EM48. The same blot was stripped and re-probed with anti-β-tubulin E7 antibody. β-Tubulin was used as a loading control. (**B**) Quantification of (A). The Xpo1 protein level was reduced in 12-week-old mice when compared with 2-week-old mice ($^*P < 0.05$, compared with 2-week-old mice, $n = 3$). Error bars represent SEM. (**C**) Western blot analysis of cytoplasmic (C) and nuclear (N) Htt protein extracted from R6/2 mice at 2 and 12 weeks of age. The reduction in Xpo1 protein level shown in (A) was accompanied by an accumulation of SDS-insoluble expanded Htt protein in the nucleus (vertical bar) as detected by anti-Htt antibody EM48. The same blot was stripped and re-probed with anti-β-tubulin E7 and anti-histone H3 antibodies.

Table 2. Subcellular localization of Q81-EGFP protein in HEK293 cells

Sucellular localization	Nucleus		Cytoplasm	
Form of Q81–EGFP protein	Diffuse	Aggregate	Diffuse	Aggregate
Average no. of cells counted	172 ± 4	200	149 ± 5	0

Two hundred cells were counted in each experiment, and a total of 600 cells were counted from three independent experiments (mean ± SD).

accumulated in the nucleus, and subsequently forming protein aggregates (Fig. 4A). This is also consistent with our subcellular fractionation results obtained from R6/2 transgenic mice that SDS-insoluble Htt protein predominantly localized to the nucleus (Fig. 7C). Our findings are in line with a previous report which showed that the reduction of cellular proteasomal activity promotes protein aggregation and accumulation of polyQ protein in the nucleus (15).

The major *in vivo* model we employed in this study is the full-length MJD (MJDQ84) disease model (24). Although functional NESs have been identified in non-polyQ regions of the MJD disease protein, those signals were found to be Xpo1 insensitive (46,47). Further, similar modulatory effect of Xpo1 was also observed in different polyQ disease models in our study (Supplementary Material, Fig. S5). We thus believe that expanded polyQ domain, the only sequence that is common to all different disease proteins, is the determinant responsible for Xpo1-mediated modification of polyQ toxicity. Both of our (Fig. 5C and D) and another study (25) showed that *Xpo1* is a genetic modifier of MJD-induced degeneration, and we further related Xpo1 function to both nuclear accumulation of expanded polyQ protein (Fig. 5A and B) and *hsp* gene induction impairment (Fig. 6A–C). Our data are also in good agreement with previous reports that nuclear localization of the expanded MJD protein is critical for disease manifestation (2), and transcriptional dysregulation is the pathogenic event commonly observed in MJD toxicity (32,50). Although over-expression of *Xpo1* attenuated early stage of MJDQ84 toxicity by prolonging the cellular heat shock response (Supplementary Material, Fig. S7), similar to *hsp70* over-expression (31) it was unable to suppress degeneration in aged flies (Supplementary Material, Fig. S10). This suggests that the continuous buildup of toxic expanded polyQ protein in the cytoplasm also causes cellular dysfunction (51,52).

Unlike Hsp70, which is able to suppress various kinds of neurotoxicity including those caused by expanded polyQ proteins and α-synuclein (Supplementary Material, Fig. S6; (29,35)), Xpo1 specifically modulated polyQ degeneration (Fig. 5, and Supplementary Material, Figs S5 and S6). Molecular chaperones, such as Hsp70, mitigate neurodegeneration by assisting the refolding of misfolded proteins in general (30). However, Xpo1 suppresses polyQ toxicity by promoting the nuclear export of expanded polyQ protein, a specific process that depends on the particular interaction between expanded polyQ protein and Xpo1 (Fig. 3 and Supplementary Material, Fig. S2). Such an interaction promotes the nuclear export of expanded polyQ proteins. Although nuclear toxicity of α-synuclein has been reported (36), it is speculated that the inability of Xpo1 to modulate α-synuclein-induced toxicity is attributed to a lack of receptor–substrate interaction between Xpo1 and α-synuclein.

In line with the progressive nature of polyQ degeneration, we demonstrated a developmental decline of Xpo1 protein levels in both wide-type and R6/2 HD transgenic mice (Fig. 7 and Supplementary Material, Fig. S9). Such observation is indeed in good agreement with the progressive decrease of Hsp70 level reported in polyQ transgenic mice (32,53–55). A decline in the Xpo1 levels results in nuclear accumulation of expanded polyQ protein, which then disrupts *hsp70* transcription through binding to its promoter (Fig. 6C), and hence leads to a reduction in the Hsp70 level. Our data obtained from the *Drosophila* MJDQ84/*ds_Xpo1* model (Figs 5 and 6) are also coherent with the mouse data (Fig. 7 and Supplementary Material, Fig. S9).

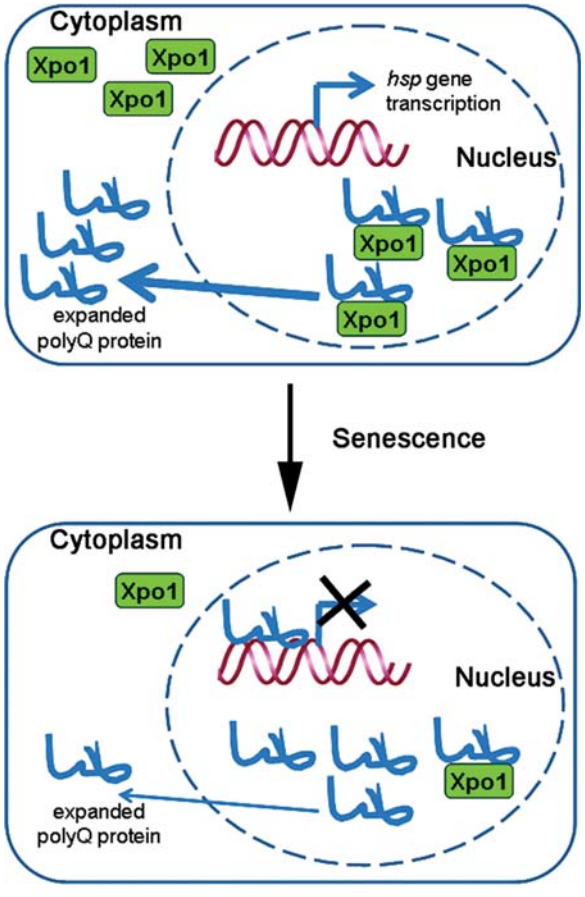

Figure 8. A proposed model for the involvement of Xpo1 in polyQ pathogenesis. Expanded polyQ protein resided in the nucleus interacts with Xpo1 and is exported out to cytoplasm. Owing to the developmental decline of Xpo1 protein level, expanded polyQ protein accumulates in the nucleus, interacts with gene promoter and hence causes transcriptional dysregulation.

Taken together, our findings all highlight an important role of Xpo1 on influencing *hsp* gene induction in polyQ pathogenesis. Therefore, a gradual temporal decline in the Xpo1 protein levels would account for the late-onset characteristics of polyQ diseases.

Figure 8 summarizes our findings in this study. Expanded polyQ domain possesses NES activity, and it interacts with Xpo1 in the nucleus to mediate polyQ protein nuclear export. Results from our fly models showed that by promoting nuclear export of expanded polyQ protein, Xpo1 helps in reducing the inhibitory effect of expanded polyQ protein on *hsp* gene induction in the nucleus. Nuclear expanded polyQ protein is capable of interacting with *hsp* promoter and hence interferes with gene transcription. Owing to the developmental decline of Xpo1 protein levels, nuclear export of expanded polyQ protein is reduced which results in its nuclear accumulation and subsequently causes *hsp* gene transcriptional dysregulation. Taken together, our findings offer a novel mechanistic explanation to how expanded polyQ protein accumulates in the nucleus and exerts neurotoxicity. This study also underscores the relation of Xpo1 expression levels and the progressive nature of polyQ degeneration.

MATERIALS AND METHODS

Molecular cloning and DNA constructs

The *pcDNA3.1-Q19-EGFP-myc* and *pcDNA3.1-Q81-EGFP-myc* constructs used were previously described in (21), and the methodology used to synthesize these constructs was described in (56). The *EGFP-polyQ* fragments were polymerase chain reaction (PCR) amplified from *pUAST-EGFP-Q27* and *pUAST-EGFP-Q76* constructs (28) and cloned into the *Drosophila* expression vector *pMT/v5-A* vector using *Kpn*I and *Not*I enzymes. For the generation of *pRev(1.4)-polyQ-EGFP* constructs, polyQ-coding DNA fragments were amplified from *pcDNA3.1-polyQ-EGFP-myc* constructs and subcloned into *pRev(1.4)-EGFP* (18) using *Bam*HI and *Age*I enzymes. The truncated *MJD* fragment was subcloned from *UAS-MJDtr* transgenic fly cDNA templates (57) into *pcDNA3.1*(+) using *Eco*RI and *Xba*I enzymes. The *Htt* fragment was subcloned from *pcDNA3FLAG-Htt1–550polyQ* constructs (a kind gift of Prof. Marcy McDonald) into *pCMV-Tag2B* using *Bam*HI and *Eco*RI enzymes.

Drosophila *BG2 cell culture*. The *Drosophila* neuronal BG2-c6 (BG2) cells were cultured in M3 medium supplemented with 10% heat-inactivated fetal bovine serum, 1% penicillin–streptomycin and 10 μg/ml insulin at 25°C. BG2 cells were co-transfected with *pMT/v5-EGFP-polyQ* and *pHSneo* using Cellfectin (Invitrogen) according to manufacturer's protocol. Stable cell lines carrying the *EGFP-polyQ* transgenes were established using 2 mg/ml G418 (Calbiochem).

The DNA templates for dsRNA synthesis were PCR amplified using the 5′ *T7* promoter sequence (5′-TAATACGACTCACTATAGGGAGA-3′) in combination with 3′ gene-specific primers. Primer sequences were adopted from the *Drosophila* RNAi Screening Center website (http://www.flyrnai.org/cgi-bin/RNAi_find_primers.pl). Double-stranded RNAs were synthesized and purified using MEGAscript *T7* kit (Ambion) and NucAway Spin Column (Ambion), respectively.

The dsRNAs were introduced into BG2 cells using the bathing method (58). After 72 h of incubation, *EGFP-polyQ* transgene expression was induced by 1 mM $CuSO_4$ and cells were cultured for another 96 h. Cells were fixed, stained (5 μM Hoechst) and observed on a TC SP5 confocal microscope (Leica). Cells showed cytoplasmic, nuclear and both cytoplasmic and nuclear aggregates were counted on a single-blinded approach. For every candidate gene, a total of 300 cells, captured from three independent experiments, were analyzed.

Mammalian cell culture

HEK293 cells were cultured at 37°C with 5% CO_2 in high glucose Dulbecco's modified Eagle medium supplemented with 10% fetal bovine serum and 1% penicillin–streptomycin. Transfection was performed with Lipofectamine 2000 (Invitrogen). For the Rev(1.4)-EGFP export assay, at 8 h post-transfection, transfected cells were treated with 5 nM cycloheximide and 100 nM LMB and incubated for 4 h. To knock down *Xpo1* expression, 10 μM siRNA (ON-TARGETplus

SMARTpool, Dharmacon) was used to transfect HEK293 cells. Cells were fixed and nuclei were labeled with Hoechst (5 μM), followed by microscopic observation on a BX51 fluorescence microscope (Olympus). At least 100 cells were monitored from each of the five independent transfections.

Drosophila stocks. Flies were raised on cornmeal medium supplemented with dry yeast. The fly strains used include *UAS-myc-MJDQ27*, *UAS-myc-MJDQ84* (24); *UAS-Xpo1-dsRNA* (National Institute of Genetics, Japan); *Xpo1 EP line E128–1A* (25); *UAS-HSPA1L* (35), *UAS-HA-ARtrQ112(s)* (26), *UAS-Htt-exon1Q93* (27), *UAS-EGF*PQ76-*FLAG* (28), *UAS-α-synuclein^{WT}* (29) and *gmr-GAL4* (Bloomington *Drosophila* Stock Center, USA). Heat shock treatment of transgenic flies was performed as previously described (31).

Pseudopupil assay

Adult fly eyes were examined as previously described (28). At least 100 ommatidia from 5 to 10 flies were used to calculate the average number of rhabdomeres per ommatidium in each of the three independent crosses.

Nucleocytoplasmic fractionation of protein samples

Frozen whole brain samples isolated from R6/2 HD transgenic mice of appropriate ages were purchased from The Jackson Laboratory. To obtain total protein lysates, thawed mouse brains or adult transgenic fly heads were homogenized in ice-cold lysis buffer (20 mM Tris–HCl, 2% SDS, 50 mM dithiothreitol) and cleared by centrifugation at 16 000*g* for 15 min at 4°C. To prepare cytoplasmic and nuclear protein fractions, thawed brains from R6/2 mice or transgenic fly heads were homogenized in fractionation buffer (10 mM Tris–HCl, 10 mM NaCl, 3 mM $MgCl_2$, 0.5% NP-40) as previously described (15). Formic acid treatment of fractionated samples was performed as previously described (59) with the protein pellets resuspended in SDS sample buffer.

Western blotting

The MJDQ27/Q84 proteins isolated from adult fly heads were detected by anti-myc antibody 9B11 (1:2500, Cell Signaling Technology). The same blots were re-probed with anti-β-tubulin E7 (1:10 000, Developmental Studies Hybridoma Bank) and anti-histone H3 (1:10 000, Abcam) antibodies to determine the purities of fractions and as loading controls. Expanded Huntingtin protein was detected by anti-Huntingtin antibody EM48 (1:250, Chemicon).

Immunoprecipitation

For immunoprecipitation, transfected cells were harvested in Xpo1-binding buffer (20 mM HEPES, 150 mM NaCl, 3 mM $MgCl_2$, 0.1% NP-40) at 48 h post-transfection. This was performed as previously described (60) using anti-myc 9B11 (1:500, Cell Signaling Technology) or anti-FLAG M2 (1:500, Sigma) antibodies. Immunoprecipitation without antibodies was used as negative control. Immunoprecipitates were analyzed by sodium dodecylsulphate-polyacrylamide gel electrophoresis (SDS–PAGE) and western blotting. Anti-Xpo1 antibody (1:1000, Calbiochem) was used to detect Xpo1 protein and the same blot was re-probed with anti-myc 71D10 (1:1000, Cell Signaling Technology) or anti-FLAG M2 (1:2500, Sigma) antibodies to show the expression of myc-tagged polyQ-EGFP or FLAG-tagged MJD and Htt proteins. Secondary antibodies used were affinity-purified goat anti-rabbit and goat anti-mouse IgG peroxidase conjugate (1:2500, Cell Signaling Technology).

Chromatin immunoprecipitation

The ChIP assay was performed on *MJDQ27*and *MJDQ84* transgenic fly lysates as previously described (61). The chromatin solutions were incubated with anti-myc 9B11 (1:250, Cell Signaling Technology) and protein A agarose overnight at 4°C. After washing, immunoprecipitates were eluted and DNA was precipitated. The pelleted DNA was re-suspended in H_2O and used as template for *hsp70* promoter PCR amplification using primers as described (62).

Size exclusion chromatography

HEK293 cells expressing either Q19– or Q81–EGFP were harvested in Xpo1-binding buffer. Size exclusion chromatography was performed using the HiPrep 26/60 Sephacryl S-300 column operated on an AKTAprime Plus System (GE Healthcare). Ferritin (440 kDa), aldolase (158 kDa) and albumin (67 kDa) were used as molecular size standards. Fractions were subjected to SDS–PAGE and western blotting using anti-Xpo1 antibody (1:1000, Calbiochem).

Confocal microscopy

Transfected HEK293 cells were fixed and stained with anti-Xpo1 (clone 17, 1:1000, BD Transduction Laboratories) and anti-survivin (1:1000, R&D Systems) antibodies, followed by tetramethylrhodamine isothiocyanate-conjugated secondary antibodies (1:250, Invitrogen). GFP fluorescence signal was used to detect Q19– and Q81–EGFP protein. After labeling the nuclei with TO-PRO-3 (1:400, Invitrogen), cell images were captured by the TC SP5 confocal system (Leica). Consistent results were obtained from three independent sets of transfection.

Reverse transcription–PCR (RT–PCR)

Total RNA extraction, conditions for RT–PCR, and the primers used in the amplification of β-*actin* and *hsp70* were essentially the same as previously described (31).

Statistical analyses

Protein bands and PCR amplicons were quantified by the Image J software (version 1.32; Research Services Branch, National Institute of Mental Health). The Kruskal–Wallis one-way ANOVA on ranks followed by Dunn post-test was performed to determine the difference in the Rev(1.4)-EGFP export assay (Fig. 2B and D). The Mann–Whitney rank sum test was performed to determine mean differences when comparing results for the nucleocytoplasmic ratio of polyQ

proteins (Fig. 5B), pseudopupil assays (Figs 5D, 6E, and Supplementary Material, Figs S6 and S10), and temporal analysis of the Xpo1 level (Fig. 7 and Supplementary Material, Fig. S9) between groups. Two-tailed, unpaired Student's *t*-test was performed to analyze the dsRNA data obtained from BG2 cells (Table 1). A *P*-value of <0.05 was considered statistically significant.

SUPPLEMENTARY MATERIAL

Supplementary Material is available at *HMG* online.

ACKNOWLEDGEMENTS

We thank Dr Cahir O'Kane, Dr Terrence Lau, Dr Sheng Zhang, Dr Bernard Mathey-Prevot, current and past members of the Laboratory of *Drosophila* Research for helpful discussion; Dr Nancy Bonini for fly stocks; Dr Beric Henderson for *pRev(1.4)-EGFP* constructs, Dr Marcy McDonald for *Huntingtin* constructs and Dr Tatsushi Toda for *polyQ-EGFP-myc* constructs.

Conflict of Interest statement. None declared.

FUNDING

This work was supported by CERG [CUHK4314/03M, CUHK4413/04M] and GRF [460908] grants from the Research Grants Council of Hong Kong, and the Hong Kong Spinocerebellar Ataxia Association.

REFERENCES

1. Orr, H.T. and Zoghbi, H.Y. (2007) Trinucleotide repeat disorders. *Annu. Rev. Neurosci.*, **30**, 575–621.
2. Bichelmeier, U., Schmidt, T., Hubener, J., Boy, J., Ruttiger, L., Habig, K., Poths, S., Bonin, M., Knipper, M., Schmidt, W.J. *et al.* (2007) Nuclear localization of ataxin-3 is required for the manifestation of symptoms in SCA3: in vivo evidence. *J. Neurosci.*, **27**, 7418–7428.
3. Klement, I.A., Skinner, P.J., Kaytor, M.D., Yi, H., Hersch, S.M., Clark, H.B., Zoghbi, H.Y. and Orr, H.T. (1998) Ataxin-1 nuclear localization and aggregation: role in polyglutamine-induced disease in SCA1 transgenic mice. *Cell*, **95**, 41–53.
4. Kordasiewicz, H.B., Thompson, R.M., Clark, H.B. and Gomez, C.M. (2006) C-termini of P/Q-type Ca^{2+} channel alpha1A subunits translocate to nuclei and promote polyglutamine-mediated toxicity. *Hum. Mol. Genet.*, **15**, 1587–1599.
5. Nucifora, F.C. Jr., Ellerby, L.M., Wellington, C.L., Wood, J.D., Herring, W.J., Sawa, A., Hayden, M.R., Dawson, V.L., Dawson, T.M. and Ross, C.A. (2003) Nuclear localization of a non-caspase truncation product of atrophin-1, with an expanded polyglutamine repeat, increases cellular toxicity. *J. Biol. Chem.*, **278**, 13047–13055.
6. Peters, M.F., Nucifora, F.C. Jr., Kushi, J., Seaman, H.C., Cooper, J.K., Herring, W.J., Dawson, V.L., Dawson, T.M. and Ross, C.A. (1999) Nuclear targeting of mutant Huntingtin increases toxicity. *Mol. Cell Neurosci.*, **14**, 121–128.
7. Saudou, F., Finkbeiner, S., Devys, D. and Greenberg, M.E. (1998), *Cell*, **95**, pp. 55–66.
8. Schilling, G., Savonenko, A.V., Klevytska, A., Morton, J.L., Tucker, S.M., Poirier, M., Gale, A., Chan, N., Gonzales, V., Slunt, H.H. *et al.* (2004) Nuclear-targeting of mutant huntingtin fragments produces Huntington's disease-like phenotypes in transgenic mice. *Hum. Mol. Genet.*, **13**, 1599–1610.
9. Schilling, G., Wood, J.D., Duan, K., Slunt, H.H., Gonzales, V., Yamada, M., Cooper, J.K., Margolis, R.L., Jenkins, N.A., Copeland, N.G. *et al.* (1999) Nuclear accumulation of truncated atrophin-1 fragments in a transgenic mouse model of DRPLA. *Neuron*, **24**, 275–286.
10. Benn, C.L., Landles, C., Li, H., Strand, A.D., Woodman, B., Sathasivam, K., Li, S.H., Ghazi-Noori, S., Hockly, E., Faruque, S.M. *et al.* (2005) Contribution of nuclear and extranuclear polyQ to neurological phenotypes in mouse models of Huntington's disease. *Hum. Mol. Genet.*, **14**, 3065–3078.
11. Jackson, W.S., Tallaksen-Greene, S.J., Albin, R.L. and Detloff, P.J. (2003) Nucleocytoplasmic transport signals affect the age at onset of abnormalities in knock-in mice expressing polyglutamine within an ectopic protein context. *Hum. Mol. Genet.*, **12**, 1621–1629.
12. Mosammaparast, N. and Pemberton, L.F. (2004) Karyopherins: from nuclear-transport mediators to nuclear-function regulators. *Trends Cell Biol.*, **14**, 547–556.
13. Tran, E.J. and Wente, S.R. (2006) Dynamic nuclear pore complexes: life on the edge. *Cell*, **125**, 1041–1053.
14. Ordway, J.M., Tallaksen-Greene, S., Gutekunst, C.A., Bernstein, E.M., Cearley, J.A., Wiener, H.W., Dure, L.S.t., Lindsey, R., Hersch, S.M., Jope, R.S. *et al.* (1997) Ectopically expressed CAG repeats cause intranuclear inclusions and a progressive late onset neurological phenotype in the mouse. *Cell*, **91**, 753–763.
15. Cornett, J., Cao, F., Wang, C.E., Ross, C.A., Bates, G.P., Li, S.H. and Li, X.J. (2005) Polyglutamine expansion of huntingtin impairs its nuclear export. *Nat. Genet.*, **37**, 198–204.
16. Taylor, J., Grote, S.K., Xia, J., Vandelft, M., Graczyk, J., Ellerby, L.M., La Spada, A.R. and Truant, R. (2006) Ataxin-7 can export from the nucleus via a conserved exportin-dependent signal. *J. Biol. Chem.*, **281**, 2730–2739.
17. Fornerod, M., Ohno, M., Yoshida, M. and Mattaj, I.W. (1997) CRM1 is an export receptor for leucine-rich nuclear export signals. *Cell*, **90**, 1051–1060.
18. Henderson, B.R. and Eleftheriou, A. (2000) A comparison of the activity, sequence specificity, and CRM1-dependence of different nuclear export signals. *Exp. Cell Res.*, **256**, 213–224.
19. Kau, T.R. and Silver, P.A. (2003) Nuclear transport as a target for cell growth. *Drug Discov. Today*, **8**, 78–85.
20. Wolff, B., Sanglier, J.J. and Wang, Y. (1997) Leptomycin B is an inhibitor of nuclear export: inhibition of nucleo-cytoplasmic translocation of the human immunodeficiency virus type 1 (HIV-1) Rev protein and Rev-dependent mRNA. *Chem. Biol.*, **4**, 139–147.
21. Popiel, H.A., Nagai, Y., Onodera, O., Inui, T., Fujikake, N., Urade, Y., Strittmatter, W.J., Burke, J.R., Ichikawa, A. and Toda, T. (2004) Disruption of the toxic conformation of the expanded polyglutamine stretch leads to suppression of aggregate formation and cytotoxicity. *Biochem. Biophys. Res. Commun.*, **317**, 1200–1206.
22. Nucifora, F.C. Jr., Sasaki, M., Peters, M.F., Huang, H., Cooper, J.K., Yamada, M., Takahashi, H., Tsuji, S., Troncoso, J., Dawson, V.L. *et al.* (2001) Interference by huntingtin and atrophin-1 with cbp-mediated transcription leading to cellular toxicity. *Science*, **291**, 2423–2428.
23. Rodriguez, J.A., Span, S.W., Ferreira, C.G., Kruyt, F.A. and Giaccone, G. (2002) CRM1-mediated nuclear export determines the cytoplasmic localization of the antiapoptotic protein Survivin. *Exp. Cell Res.*, **275**, 44–53.
24. Warrick, J.M., Morabito, L.M., Bilen, J., Gordesky-Gold, B., Faust, L.Z., Paulson, H.L. and Bonini, N.M. (2005) Ataxin-3 suppresses polyglutamine neurodegeneration in *Drosophila* by an ubiquitin-associated mechanism. *Mol. Cell*, **18**, 37–48.
25. Bilen, J. and Bonini, N.M. (2007) Genome-wide screen for modifiers of ataxin-3 neurodegeneration in Drosophila. *PLoS Genet.*, **3**, 1950–1964.
26. Chan, H.Y., Warrick, J.M., Andriola, I., Merry, D. and Bonini, N.M. (2002) Genetic modulation of polyglutamine toxicity by protein conjugation pathways in *Drosophila*. *Hum. Mol. Genet.*, **11**, 2895–2904.
27. Steffan, J.S., Bodai, L., Pallos, J., Poelman, M., McCampbell, A., Apostol, B.L., Kazantsev, A., Schmidt, E., Zhu, Y.Z., Greenwald, M. *et al.* (2001) Histone deacetylase inhibitors arrest polyglutamine-dependent neurodegeneration in *Drosophila*. *Nature*, **413**, 739–743.
28. Wong, S.L., Chan, W.M. and Chan, H.Y. (2008) Sodium dodecyl sulfate-insoluble oligomers are involved in polyglutamine degeneration. *FASEB J.*, **22**, 3348–3357.
29. Auluck, P.K., Chan, H.Y., Trojanowski, J.Q., Lee, V.M. and Bonini, N.M. (2002) Chaperone suppression of alpha-synuclein toxicity in a *Drosophila* model for Parkinson's disease. *Science*, **295**, 865–868.

30. Muchowski, P.J. and Wacker, J.L. (2005) Modulation of neurodegeneration by molecular chaperones. *Nat. Rev. Neurosci.*, **6**, 11–22.
31. Huen, N.Y. and Chan, H.Y. (2005) Dynamic regulation of molecular chaperone gene expression in polyglutamine disease. *Biochem. Biophys. Res. Commun.*, **334**, 1074–1084.
32. Chou, A.H., Yeh, T.H., Ouyang, P., Chen, Y.L., Chen, S.Y. and Wang, H.L. (2008) Polyglutamine-expanded ataxin-3 causes cerebellar dysfunction of SCA3 transgenic mice by inducing transcriptional dysregulation. *Neurobiol. Dis.*, **31**, 89–101.
33. Hands, S., Sinadinos, C. and Wyttenbach, A. (2008) Polyglutamine gene function and dysfunction in the ageing brain. *Biochim. Biophys. Acta*, **1779**, 507–521.
34. Benn, C.L., Sun, T., Sadri-Vakili, G., McFarland, K.N., DiRocco, D.P., Yohrling, G.J., Clark, T.W., Bouzou, B. and Cha, J.H. (2008) Huntingtin modulates transcription, occupies gene promoters in vivo, and binds directly to DNA in a polyglutamine-dependent manner. *J. Neurosci.*, **28**, 10720–10733.
35. Warrick, J.M., Chan, H.Y., Gray-Board, G.L., Chai, Y., Paulson, H.L. and Bonini, N.M. (1999) Suppression of polyglutamine-mediated neurodegeneration in *Drosophila* by the molecular chaperone HSP70. *Nat. Genet.*, **23**, 425–428.
36. Kontopoulos, E., Parvin, J.D. and Feany, M.B. (2006) Alpha-synuclein acts in the nucleus to inhibit histone acetylation and promote neurotoxicity. *Hum. Mol. Genet.*, **15**, 3012–3023.
37. Mangiarini, L., Sathasivam, K., Seller, M., Cozens, B., Harper, A., Hetherington, C., Lawton, M., Trottier, Y., Lehrach, H., Davies, S.W. *et al.* (1996) Exon 1 of the HD gene with an expanded CAG repeat is sufficient to cause a progressive neurological phenotype in transgenic mice. *Cell*, **87**, 493–506.
38. Davies, S.W., Turmaine, M., Cozens, B.A., DiFiglia, M., Sharp, A.H., Ross, C.A., Scherzinger, E., Wanker, E.E., Mangiarini, L. and Bates, G.P. (1997) Formation of neuronal intranuclear inclusions underlies the neurological dysfunction in mice transgenic for the HD mutation. *Cell*, **90**, 537–548.
39. Havel, L.S., Li, S. and Li, X.J. (2009) Nuclear accumulation of polyglutamine disease proteins and neuropathology. *Mol. Brain*, **2**, 21.
40. Bessert, D.A., Gutridge, K.L., Dunbar, J.C. and Carlock, L.R. (1995) The identification of a functional nuclear localization signal in the Huntington disease protein. *Brain Res. Mol. Brain Res.*, **33**, 165–173.
41. Chen, S., Peng, G.H., Wang, X., Smith, A.C., Grote, S.K., Sopher, B.L. and La Spada, A.R. (2004) Interference of Crx-dependent transcription by ataxin-7 involves interaction between the glutamine regions and requires the ataxin-7 carboxy-terminal region for nuclear localization. *Hum. Mol. Genet.*, **13**, 53–67.
42. Jenster, G., Trapman, J. and Brinkmann, A.O. (1993) Nuclear import of the human androgen receptor. *Biochem. J.*, **293** (Pt 3), 761–768.
43. Kaytor, M.D., Duvick, L.A., Skinner, P.J., Koob, M.D., Ranum, L.P. and Orr, H.T. (1999) Nuclear localization of the spinocerebellar ataxia type 7 protein, ataxin-7. *Hum. Mol. Genet.*, **8**, 1657–1664.
44. Saporita, A.J., Zhang, Q., Navai, N., Dincer, Z., Hahn, J., Cai, X. and Wang, Z. (2003) Identification and characterization of a ligand-regulated nuclear export signal in androgen receptor. *J. Biol. Chem.*, **278**, 41998–42005.
45. Xia, J., Lee, D.H., Taylor, J., Vandelft, M. and Truant, R. (2003) Huntingtin contains a highly conserved nuclear export signal. *Hum. Mol. Genet.*, **12**, 1393–1403.
46. Antony, P.M., Mantele, S., Mollenkopf, P., Boy, J., Kehlenbach, R.H., Riess, O. and Schmidt, T. (2009) Identification and functional dissection of localization signals within ataxin-3. *Neurobiol Dis.*, **36**, 280–292.
47. Macedo-Ribeiro, S., Cortes, L., Maciel, P. and Carvalho, A.L. (2009) Nucleocytoplasmic shuttling activity of ataxin-3. *PLoS One*, **4**, e5834.
48. Walsh, R., Storey, E., Stefani, D., Kelly, L. and Turnbull, V. (2005) The roles of proteolysis and nuclear localisation in the toxicity of the polyglutamine diseases. A review. *Neurotox. Res.*, **7**, 43–57.
49. Kudo, N., Matsumori, N., Taoka, H., Fujiwara, D., Schreiner, E.P., Wolff, B., Yoshida, M. and Horinouchi, S. (1999) Leptomycin B inactivates CRM1/exportin 1 by covalent modification at a cysteine residue in the central conserved region. *Proc. Natl Acad. Sci. USA*, **96**, 9112–9117.
50. Evert, B.O., Araujo, J., Vieira-Saecker, A.M., de Vos, R.A., Harendza, S., Klockgether, T. and Wullner, U. (2006) Ataxin-3 represses transcription via chromatin binding, interaction with histone deacetylase 3, and histone deacetylation. *J. Neurosci.*, **26**, 11474–11486.
51. Gunawardena, S., Her, L.S., Brusch, R.G., Laymon, R.A., Niesman, I.R., Gordesky-Gold, B., Sintasath, L., Bonini, N.M. and Goldstein, L.S. (2003) Disruption of axonal transport by loss of huntingtin or expression of pathogenic polyQ proteins in *Drosophila*. *Neuron*, **40**, 25–40.
52. Wang, C.E., Zhou, H., McGuire, J.R., Cerullo, V., Lee, B., Li, S.H. and Li, X.J. (2008) Suppression of neuropil aggregates and neurological symptoms by an intracellular antibody implicates the cytoplasmic toxicity of mutant huntingtin. *J. Cell Biol.*, **181**, 803–816.
53. Hay, D.G., Sathasivam, K., Tobaben, S., Stahl, B., Marber, M., Mestril, R., Mahal, A., Smith, D.L., Woodman, B. and Bates, G.P. (2004) Progressive decrease in chaperone protein levels in a mouse model of Huntington's disease and induction of stress proteins as a therapeutic approach. *Hum. Mol. Genet.*, **13**, 1389–1405.
54. Yamanaka, T., Miyazaki, H., Oyama, F., Kurosawa, M., Washizu, C., Doi, H. and Nukina, N. (2008) Mutant Huntingtin reduces HSP70 expression through the sequestration of NF-Y transcription factor. *Embo J.*, **27**, 827–839.
55. Merienne, K., Helmlinger, D., Perkin, G.R., Devys, D. and Trottier, Y. (2003) Polyglutamine expansion induces a protein-damaging stress connecting heat shock protein 70 to the JNK pathway. *J. Biol. Chem.*, **278**, 16957–16967.
56. Onodera, O., Burke, J.R., Miller, S.E., Hester, S., Tsuji, S., Roses, A.D. and Strittmatter, W.J. (1997) Oligomerization of expanded-polyglutamine domain fluorescent fusion proteins in cultured mammalian cells. *Biochem. Biophys. Res. Commun.*, **238**, 599–605.
57. Warrick, J.M., Paulson, H.L., Gray-Board, G.L., Bui, Q.T., Fischbeck, K.H., Pittman, R.N. and Bonini, N.M. (1998) Expanded polyglutamine protein forms nuclear inclusions and causes neural degeneration in Drosophila. *Cell*, **93**, 939–949.
58. Clemens, J.C., Worby, C.A., Simonson-Leff, N., Muda, M., Maehama, T., Hemmings, B.A. and Dixon, J.E. (2000) Use of double-stranded RNA interference in *Drosophila* cell lines to dissect signal transduction pathways. *Proc. Natl Acad. Sci. USA*, **97**, 6499–6503.
59. Lam, W., Chan, W.M., Lo, T.W., Wong, A.K., Wu, C.C. and Chan, H.Y. (2008) Human receptor for activated protein kinase C1 associates with polyglutamine aggregates and modulates polyglutamine toxicity. *Biochem. Biophys. Res. Commun.*, **377**, 714–719.
60. Hakata, Y., Yamada, M., Mabuchi, N. and Shida, H. (2002) The carboxy-terminal region of the human immunodeficiency virus type 1 protein Rev has multiple roles in mediating CRM1-related Rev functions. *J. Virol.*, **76**, 8079–8089.
61. Aparicio, O., Geisberg, J.V., Sekinger, E., Yang, A., Moqtaderi, Z. and Struhl, K. (2005) Chromatin immunoprecipitation for determining the association of proteins with specific genomic sequences in vivo. *Curr. Protoc. Mol. Biol.*, Chapter 21, Unit 21 23.
62. Imbriano, C., Bolognese, F., Gurtner, A., Piaggio, G. and Mantovani, R. (2001) HSP-CBF is an NF-Y-dependent coactivator of the heat shock promoters CCAAT boxes. *J. Biol. Chem.*, **276**, 26332–26339.